ORIGINAL RESEARCH

# Inhibition of Ca2+ induced Macrophage Oxidative Stress Cascade in Mice With Ulcerative Colitis

Hao Yan, MM; Guohong Li, MD


## ABSTRACT

**Context** • In the context of ulcerative coloproctitis (UC), a chronic and non-specific inflammatory condition of the colon and rectum with an elusive etiology, the therapeutic potential of G protein-coupled receptor 109a (GPR109a) has gained prominence. GPR109a is expressed in various cell types including colonic epithelium, adipocytes, neutrophils, and macrophages, positioning it as a promising candidate for pharmacological intervention in colitis.

**Objective** • the mechanistic role of GPR109a in a mouse model of UC and to assess its capacity to mitigate the disease's progression.

**Design** • The research team performed an animal study.

**Setting** • Conducted by a research team in the biomedical setting of the People's Hospital of Dongxihu District in Wuhan, Hubei province of China.

**Animals** • This animal study engaged 16 specific pathogen-free (SPF) male BALB/c mice, aged between 4 to 6 weeks and weighing 20-24 grams each.

**Outcome Measures** • (1) analysis of rectal lesions via hematoxylin-eosin (HE) staining, (2) the use of transmission electron microscopy to examine suborganelle spatial relationships, (3) Western blot analysis to evaluate a spectrum of protein expressions such as phosphorylated IP3R, p-PERK, p-IRE-1α, mitofusins, NADPH oxidases, TNF-α, and IL-1β, and (4) determination of intracellular calcium concentrations to gauge intestinal barrier function impairment involving specific calcium pathway signals.

**Results** • Results from the study painted a picture of significant infiltration by inflammatory cells within the mucosal and submucosal layers, compounded by pronounced endoplasmic reticulum expansion. Abundant interfaces between the ER and the mitochondria formed multiple structures known as mitochondria-associated membranes or MAMs. When evaluated under calcium-rich conditions, the protein levels mentioned earlier were notably elevated in the GPR109a knockdown (KD) group versus the infection control (NC) counterparts. However, this differential expression disappeared under calcium-depleted conditions or when treated with 2-aminoethyl diphenyl borinate (2-APB). Additionally, fluorescence intensity assays showed marked suppression in the GPR109a-KD plus lipopolysaccharide (LPS) group compared to the control.

**Conclusions** • Drawing these observations to a close, the study concluded that GPR109a has an inhibitory effect on the advancement of ulcerative coloproctitis in mice. This is mediated through the activation of a calcium-induced oxidative stress cascade within macrophages, delineating a promising therapeutic pathway for the management of this inflammatory disease. (*Altern Ther Health Med.* 2024;30(12):222-229).


**Hao Yan**, MM, Attending Physician; **Guohong Li**, MD, Attending Physician, Department of Gastroenterology; People's Hospital of Dongxihu District; Wuhan, Hubei; P.R. China.

*Corresponding author: Guohong Li, MD*
*E-mail: guohongli37@hotmail.com*

## INTRODUCTION

### Ulcerative coloproctitis

Ulcerative coloproctitis (UC) is a persistently recurring inflammatory disorder that primarily afflicts the mucosal and submucosal layers of the colon and rectum, predominately targeting young and middle-aged adults.[1] This condition is characterized by localized inflammation that commonly initiates within the rectum and extends to involve the adjacent sigmoid and descending segments of the colon. An upward trend in the incidence of UC underscores an emergent health concern, particularly among individuals aged 20-40 years.[2] The evolution of UC is insidious, tending towards a protracted and intractable clinical trajectory, thereby complicating its management regime.[3] The hallmark clinical manifestations of UC include persistent diarrhea, abdominal discomfort, and the discharge of mucoid, often bloody, stools. The disease exhibits a heterogeneous severity profile and typically follows an intermittent and chronic disease pattern.[4] UC's pathogenesis is multifactorial, influenced by genetic predispositions, immune responses,

and environmental factors, and its precise etiology remains elusive. Nevertheless, chronic or unresolved endoplasmic reticulum stress has been implicated in the pathophysiology of UC, with consequences such as apoptosis and ongoing inflammation, which are central to the disease's pathology.

### Endoplasmic Reticulum

The endoplasmic reticulum (ER) is an organelle of exquisite sensitivity to cellular perturbations. Its role as an intracellular calcium store is vital for the equilibrium of calcium ions within the cell. Dysregulation of this balance, through intracellular calcium surges and oxidative stresses instigated by extraneous factors, can precipitate ER dysfunction and engender ER stress.[5] ER stress is a cellular reaction to the accumulation of unfolded proteins and calcium disequilibrium within the ER, which triggers adaptive responses such as the unfolded protein response (UPR), the overload of ER, and caspase-12-mediated apoptotic pathways.[6] During the course of ER stress, the activation of two pivotal ER sensors occurs protein kinase RNA-like ER kinase (PERK) and inositol-requiring enzyme 1 alpha (IRE-1α).[7] PERK functions as an integral transmembrane sensor within the mammalian ER, playing a critical role in the UPR. IRE1, with its two isoforms - IRE-1α and IRE-1β, is a type I transmembrane protein integral to the ER. The simultaneous activation of PERK and IRE-1α leads to the formation of a specialized interface known as the mitochondria-associated ER membrane (MAM), a structural domain that serves as a nexus between the mitochondria and the ER.

### Inositol 1,4,5-Triphosphate Receptor Enhancement

The Inositol 1,4,5-triphosphate receptor (IP3R), an essential conductor in the symphony of calcium release, plays a pivotal role as a prime calcium channel woven into the fabric of the endoplasmic reticulum (ER) membrane. Fundamental to the nuanced interplay of cellular activity, the IP3R, upon excessive activation, can unleash a cascade of disturbances within the ER.[8] This scenario entails an uncontrolled efflux of calcium from the ER to the cytosol, triggering an elevation in cytosolic calcium, overwhelming the mitochondria's calcium handling capacities, and depleting ER calcium reserves. The result may be an ominous prelude to cellular demise by way of apoptotic and necrotic pathways.

In the face of ER stress, the protein IRE1 responds as a molecular sentinel, initiating a stress-relief operation by forming dimers and activating via phosphorylation. This enables IRE1 to meticulously edit the mRNA transcript of X-box binding protein-1 (XBP-1), excising a precise 26-nucleotide segment to assemble the functional XBP-1 protein—a master regulator in the cellular stress response.[9] Active XBP-1 then proceeds to the nucleus, spearheading efforts to restore the equilibrium by enhancing proper protein folding and rapidly clearing misfolded proteins via an upsurge in molecular chaperone production. Additionally, an ignited IRE1α brandishes the ability to selectively decompose certain mRNAs through a facilitative IRE1-dependent decay (RIDD) mechanism, contributing significantly to the mitigation of ER stress.[9] Concurrently, under stressful conditions, PERK engages in a phosphorylation relay with eukaryotic initiation factor-2 alpha (eIF2α), facilitated by mitofusin 1 (MFN1) and MFN2,[10] commanding the ER to collaborate closely with the mitochondria to construct mitochondria-associated ER membrane (MAM) assemblages.

### Therapeutic Potential of G Protein-Coupled Receptor 109a

Within the diverse landscapes of the colonic epithelium, adipocytes, neutrophils, and macrophages, the G protein-coupled receptor 109a (GPR109a) operates with precision.[11] As an SCFA receptor, it directs the flow of extracellular calcium ions (Ca2+), strategically curbing the phosphorylation of IP3R, thus fine-tuning the intricate intracellular calcium signaling dance, with broad implications for cell function. GPR109a emerges as a guardian of intestinal epithelial cells, shielding them against the tides of apoptosis.[12]

At the crossroads of immunomodulation, GPR109a shines particularly in maintaining the equilibrium of the intestinal ecosystem, modulating gut-related allergies, and combatting associated disorders. Through a compelling dextran sulfate sodium (DSS)-induced colitis model, it has been shown that GPR109a signaling rallies colonic dendritic cells and macrophages to manifest their anti-inflammatory prowess, curbing the advance of colitis.[13] In stark contrast, a reduction in GPR109a expression can exacerbate colitis's progression. Niacin proudly serves as a beneficial vitamin, and beyond its nutritional benefits, at medicinal dosages, it moonlights as a GPR109A agonist, adeptly modulating the lipid panorama within the bloodstream. Singh and colleagues underscore the promise of GPR109a, hailing it as a promising therapeutic landmark for the pharmacological conquest of colitis.[14]

Building upon these insights, the current investigation is methodically devised to scrutinize the intricacies of GPR109a's influence on ulcerative coloproctitis (UC) within a murine paradigm, probing its potential to arrest the onslaught of this challenging condition, thus shedding light on novel avenues for intervention.

## METHODS

### Animals

To advance medical sciences, an animal study was meticulously conducted by the esteemed research team at the People's Hospital of Dongxihu District in Wuhan, Hubei, People's Republic of China. The study utilized a cohort of sixteen specific-pathogen-free (SPF) male BALB/c mice, carefully selected within an age range of 4 to 6 weeks and weighing between 20 to 24 grams, sourced from Beijing HFK Bioscience Co., Ltd., Beijing, China. The Department of Gastroenterology of the People's Hospital of Dongxihu District responsibly acclimatized the mice to their new conditions for one week before commencing the actual study. The living environment for these nude mice was optimized with a constant temperature of 25 degrees Celsius and a

relative humidity of 60%. The diet provided was rich in protein and low in fiber, accompanied by ad libitum access to purified drinking water. To align with their natural circadian rhythms, a cycle of 12 hours of light followed by 12 hours of darkness was sustained. The upkeep of the rodents' habitat was impeccable, endorsing cleanliness and sanitation with routine disposal of waste to mitigate any potential transmission of diseases or infection risks.

**Procedures**

The researchers adeptly established an inflammatory in vitro model using RAW264.7 cells, which they stimulated with bacterial endotoxin, and lipopolysaccharide (LPS) (CS0158, G-CLONE, Beijing, China). This agent is known for its ability to activate pivotal pathways such as toll-like receptor-4 (TLR4), nuclear factor-kappa beta (NF-κB), and mitogen-activated protein kinase (MAPK) signaling, thus modulating an array of inflammation-linked target genes like TNF-α, IL-1β, IL-6, monocyte chemoattractant protein-1 (MCP-1), inducible nitric oxide synthase (iNOS), and cyclooxygenase-2 (COX-2). Recognized for their efficacy, LPSs have become a standard inflammatory stimulus to replicate ulcerative colitis (UC) models in vitro, initiating a cellular cascade that results in the production and release of pro-inflammatory factors.

The research team diligently categorized the RAW264.7 cells into distinct experimental groups: (1) GPR109a-NC and GPR109a-KD, (2) GPR109a-NC+LPS and GPR109a-KD+LPS, (3) GPR109a-NC+LPS+DMEM calcium-free medium and GPR109a-KD+LPS+DMEM calcium-free medium (YC-2067, Shanghai Yuchun Biology Science and Technology, Shanghai, China), and (4) GPR109a-NC+LPS+2-aminoethyl diphenyl borinate (2-APB) and GPR109a-KD+LPS+2-APB (an IP3R inhibitor, HY-W009724, MedChemExpress, Monmouth Junction, New Jersey, USA).

For the mouse model establishment, the dedicated team induced ulcerative colitis in mice through the DSS free-drinking approach (160110, MP Biomedical, Santa Ana, California, USA). They carefully prepared a 3.5% DSS solution in distilled water, ensuring a daily provision of fresh solution. The researchers impartially divided the mice into two groups, GPR109a-NC and GPR109a-KD with eight mice per group, employing the random number table method. Each group of mice had unrestricted access to the DSS solution for a continuous period of seven days, followed by respective intravenous injections of lentiviral vectors encoding for either GPR109a-NC or GPR109a-KD (at a dosage of 1×10^7 PFU per mouse). Subsequent microscopic examination of their colon specimens revealed identifiable pathological markers indicative of successful model creation.

**Outcome measures**

With scientific rigor, the research team evaluated the following outcome variables: (1) the rectal lesion area with the use of hematoxylin-eosin (HE) staining, (2) the nuanced architecture of sub organelles through transmission electron microscopy, and (3) the expression levels of various proteins involved in pathophysiological processes, such as phosphorylated inositol 1,4,5-triphosphate receptor (p-IP3R), phosphorylated protein kinase RNA-like endoplasmic reticulum kinase (p-PERK), phosphorylated inositol-requiring enzyme 1/endoplasmic reticulum to nucleus 1 alpha (p-IRE-1α), MFN1, MFN2, NADPH oxidase 2 (NOX2), and NOX4, TNF-α, and IL-1β, utilizing Western blot analysis. Moreover, they determined the intracellular calcium concentrations, a notable marker of intestinal-barrier function impairment in the GPR109a-KD group, by probing the associated signaling pathways of p-IP3R/ p-PERK/ p-IRE1α and MFN2/ NADPH oxidase 4 (NOX4)/ interleukin-1 beta (IL-1β) calcium ions.

**Outcome Measures**

**Hematoxylin and Eosin (HE) Staining**. The investigative team embarked on a meticulous process where they (1) procured ulcerative coloproctitis tissue samples from mice and fashioned paraffin-embedded tissue sections. Subsequently, (2) they conducted routine deparaffinization and hydration, followed by HE staining. The detailed procedure involved (1) immersion of the sections in diluted ammoniated water for 12 hours, followed by thorough rinsing with clean water for 10 minutes. The sections were then stained with hematoxylin solution (G1004, Wuhan Servicebio Technology, Wuhan, China) for 15 minutes and subjected to a reversal bluing in diluted ammonia water for 10 minutes; (2) application of eosin staining solution (G1001, Wuhan Servicebio Technology) for one minute, immediately followed by a quick rinse with 95% ethanol; and (3) a gradient ethanol dehydration, clearing in xylene, and mounting with neutral balsam.

**Transmission Electron Microscopy**

The research contingent (1) procured fresh tissue specimens and placed them promptly into a specialized electron microscopy fixative at 4°C for 2-4 hours; (2) washed the samples thrice with 0.1mol/L phosphate-buffered saline (PBS), each for 15 minutes, at pH 7.4; (3) fixed the samples with 1% osmium tetroxide in 0.1mol/L PBS at room temperature for 2 hours; followed by (4) another set of thorough PBS washes. The samples underwent dehydration and infiltration where they were (1) immersed in a 1:1 mixture of acetone and 812 resin for 2-4 hours, followed by (2) a 2:1 mixture overnight, and finally (3) enveloped in pure 812 resin for 5-8 hours. The samples were then embedded in 812 resin within an embedding mold and cured at 37°C overnight. After polymerization, ultrathin sections were cut, stained, and examined under a transmission electron microscope (HT7700, Hitachi, Tokyo, Japan), with resulting images meticulously captured and analyzed.

**Western Blot**

The research cadre isolated and treated CD68+ cells from two mouse cohorts, namely the GPR109a-NC and

GPR109a-KD groups, alongside their respective RAW264.7 cells. They then added RIPA lysis buffer (P0013K, Jiangsu Beyotime Biotechnology, Nanjing, Jiangsu) to the cell solutions, centrifuged to discard the supernatant, and used a BCA protein assay kit (PC0020, Beijing Solarbio Science & Technology, Wuhan, China) for protein quantification. The separated proteins, after SDS-PAGE at 110 V for 2 hours, were transferred to PVDF membranes (IPVH20200, Millipore, Billerica, Massachusetts, USA).

The membranes were blocked with 5% milk before being probed with a slew of primary antibodies, including those against GPR109a, p-IP3R, p-PERK, p-IRE1α, MFN1, MFN2, NOX2, NOX4, TNF-α, IL-1β, and GAPDH, all acquired from reputable suppliers such as Thermo Fisher Scientific and Abcam. Following an overnight incubation at 4°C, the membranes were rinsed and incubated with suitable secondary antibodies. The protein signals were visualized using an advanced ECL system (Solarbio, Beijing, China), and ImageJ software facilitated the quantitative analysis of protein band intensities.

### Immunofluorescence Staining

For immunofluorescence staining, RAW264.7 cells underwent standard preparation, which included loading with Fura-2/AM (S1052, Jiangsu Beyotime Biotechnology, Nanjing, Jiangsu, China) at a final concentration of 2 μmol and incubated under light-protected conditions for approximately 50 minutes. Post incubation, the cells were centrifuged and thoroughly washed to remove any trace extracellular Fura-2, followed by resuspension in a calcium-free solution. Fluorescence measurements were taken with an RF5000 fluorescence spectrophotometer (Shimadzu Corporation, Kyoto, Japan), with excitation and emission wavelengths set at 340 nm and 510 nm, respectively. For fluorescence imaging, the cells adhered to slides were washed, fixed, and permeabilized. The application of blocking serum was followed by overnight incubation with primary antibodies, subsequent application of fluorescently labeled secondary antibodies, counterstaining with DAPI, and final mounting before visualization under a fluorescence microscope.

### Statistical Analysis

The data was systematically processed and analyzed by the team using GraphPad Prism 9.3.1 (San Diego, California, USA). For quantitative insights, continuous data was encapsulated as means ± standard deviations (SDs). To discern differences, one-way analysis of variance (ANOVA) was employed for multi-group comparisons, supplemented by the *t* test for dual-group analysis. A *P* value threshold of less than .05 was stipulated for statistical significance.

## RESULT

### Alleviation of Pathological Changes in Colon Tissue

Upon histological examination using hematoxylin and eosin (HE) staining, the colonic crypts in the GPR109a

**Figure 1.** Attenuation of Colonic Pathological Alterations in Mice by GPR109a. Hematoxylin and eosin (H&E) staining reveals the histological architecture of colonic tissue obtained from mice within the GPR109a-negative control (GPR109a-NC) cohort (as depicted in Figure 1A) and the GPR109a-knockdown (GPR109a-KD) cohort (as depicted in Figure 1B).

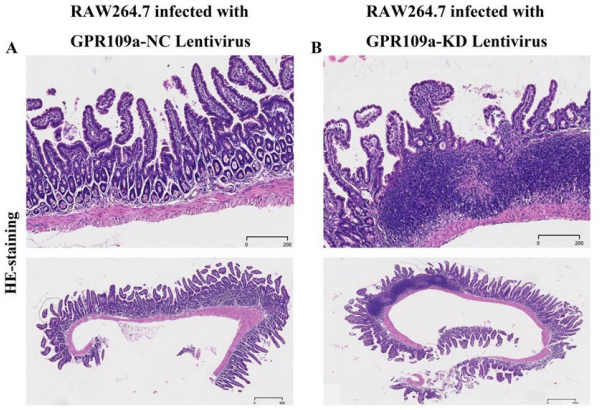


**Abbreviations:** GPR109a, G protein-coupled receptor 109a; HE, hematoxylin-eosin; KD, knockdown; NC, infection control

negative control (NC) group appeared deformed and shorter, yet maintained structural integrity. Despite the loosely arranged goblet cells and evidence of inflammatory infiltration in localized tissues (Figure 1A), the overall architecture remained relatively preserved. Conversely, the GPR109a knockdown (KD) group revealed a disrupted intestinal barrier with a significant loss of over 75% of goblet cells and pronounced infiltration of inflammatory cells within the mucosal layer and submucosa. Furthermore, the disappearance of numerous crypts in the KD group suggested a more severe disruption compared to the NC group (Figure 1B). Importantly, the comparison between the two groups highlights the potential role of GPR109a in mitigating the pathological alterations within mouse colon tissue.

### Improvement in Lesion Progression

Transmission electron microscopy unveiled various degrees of structural compromise in the GPR109a-NC group, which included a moderately degraded colon-intestinal barrier, disorganized and sparsely distributed microvilli, and instances of microvilli shedding. Additional findings included a slight dilation of the rough endoplasmic reticulum, the presence of autophagolysosomes, and minimal mitochondrial-associated membrane (MAM) structures (Figure 2A).

In comparison, the GPR109a-KD group's electron microscopic analysis indicated a more pronounced preservation of the colon-intestinal barrier despite observable damage. This included partial epithelial-cell disintegration, widespread cell-membrane damage with large-scale matrix degradation, and substantial loss of microvilli, highlighting the severity of lesion progression. Enlargement and expansion of the rough endoplasmic reticulum were significant, coupled with an increase in autophagolysosomes. Notably, the proximity between the endoplasmic reticulum and

**Figure 2.** Amelioration of Colonic Lesion Progression in Mice by GPR109a. Electron microscopy images exhibit the ultrastructural details of murine colonic tissues at magnifications of 12,000× and 6,000× for the GPR109a-NC group (displayed in Figure 2A) and GPR109a-KD group (displayed in Figure 2B), respectively. Notably, the black arrows within the images demarcate the mitochondria-associated endoplasmic reticulum membranes (MAMs).

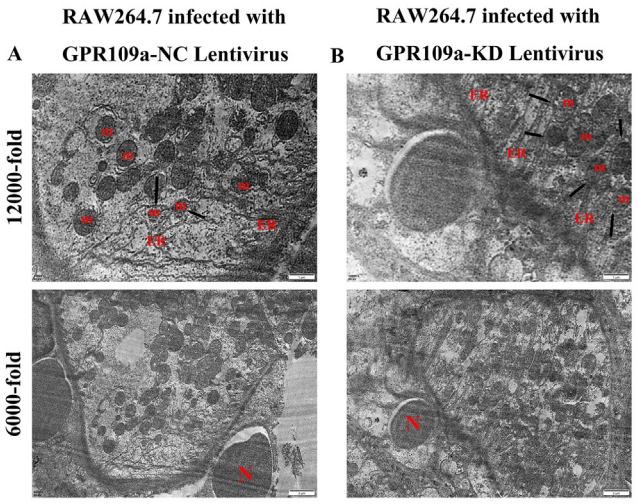


**Abbreviations:** GPR109a, G protein-coupled receptor 109a; KD, knockdown; NC, infection control; ER, endoplasmic reticulum; N, nucleus; m, mitochondria

**Figure 3.** Suppression of Inflammatory Progression via GPR109a-Mediated Induction of Macrophage Protein Expression. Immunoblotting analyses depicting protein expression profiles within macrophages from murine colonic tissue are presented in Figure 3A for both experimental cohorts. Correspondingly, Figure 3B illustrates a quantitative evaluation of the protein expression levels in the aforementioned macrophages, with data represented as mean values accompanied by the standard deviation.

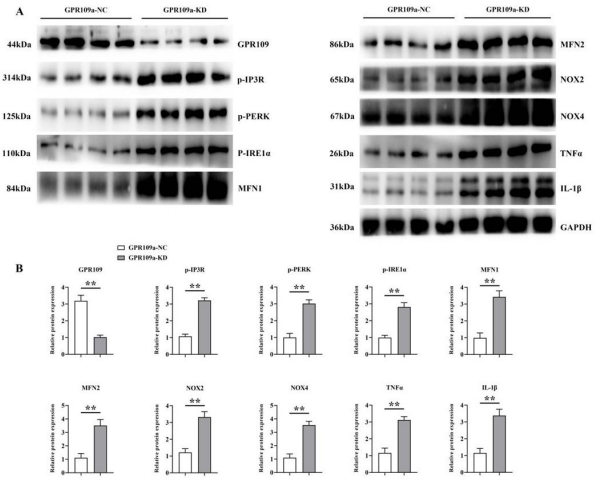


*$P < .01$, indicating that the expression level of GPR109a protein in the GPR109A-KD group was significantly lower than that of the GPR109A-NC group and the expression levels of p-IP3R, p-PERK, p-IRE-1α, MFN1, MFN2, NOX2, NOX4, TNF-α, and IL-1β proteins in GPR109a-KD group were significantly higher than those of the GPR109a-NC group

**Abbreviations:** GPR109a, G protein-coupled receptor 109a; IL-1β, interleukin-1 beta; KD, knockdown; MFN1, mitofusin 1; MFN2, mitofusin 2; NC, infection control; NOX2, nicotinamide adenine dinucleotide phosphate (NADPH) oxidase 2; NOX4, nicotinamide adenine dinucleotide phosphate (NADPH) oxidase 4; p-IP3R, phosphorylated inositol 1,4,5-triphosphate receptor; p-IRE-1α, phosphorylated inositol-requiring enzyme1/endoplasmic reticulum to nucleus1 alpha; p-PERK, phos2phorylated protein kinase RNA-like endoplasmic reticulum kinase; TNF-α, tumor necrosis factor alpha

mitochondria, forming numerous MAMs (Figure 2B), suggested a stress response that was less evident in the NC group. These observations suggest that GPR109a expression may reduce the progression of lesions in the colon by maintaining membrane and ultrastructural integrity.

### Inhibition of Inflammation by GPR109a

Western blot analyses revealed that protein expression levels of GPR109a were significantly reduced in the GPR109a-KD group compared to the NC group ($P < .01$). Further, the KD group displayed elevated levels of pro-inflammatory and

**Figure 4.** Modulation of Inflammatory Pathways by GPR109a through Augmentation of Intracellular Ca2+ Concentrations in Macrophages. Presented are the images reflecting Ca2+ immunofluorescence staining in various cellular cohorts: GPR109a negative control (GPR109a-NC) cells (Figure 4A), GPR109a-knockdown (GPR109a-KD) cells (Figure 4B), GPR109a-NC cells treated with lipopolysaccharide (LPS) (Figure 4C), GPR109a-KD cells with LPS treatment (Figure 4D), GPR109a-NC cells in LPS and calcium-free media (Figure 4E), and GPR109a-KD cells in LPS and calcium-free media (Figure 4F). Figure 4G quantitatively assesses the relative fluorescence intensities representing intracellular Ca2+ levels across the different cellular conditions, with data expressed as means ± standard deviations.

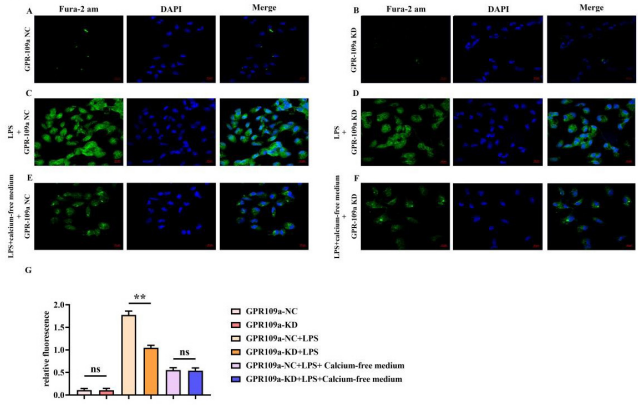


*$P$ < .01, indicating that the GPR109a-NC+LPS group's relative fluorescence intensity was significantly higher than that of GPR109a-KD+LPS group

**Abbreviations:** DAPI, 4',6-diamidino-2-phenylindole; Fura-2/AM, fura-2 acetoxymethyl ester; GPR109a, G protein-coupled receptor 109a; KD, knockdown; LPS, lipopolysaccharide; NC, infection control; ns, no significance

**Figure 5.** Regulation of Inflammatory Progression Through GPR109a-Induced Protein Expression in Macrophages and the Ca2±Triggered Oxidative Stress Response In Vitro. The protein expression profiles of macrophages across different experimental groups, as determined by Western blot analysis, are shown in Figure 5A. The comparative expression levels of these proteins are graphically represented in Figure 5B, with quantitative data illustrated as means ± standard deviations.

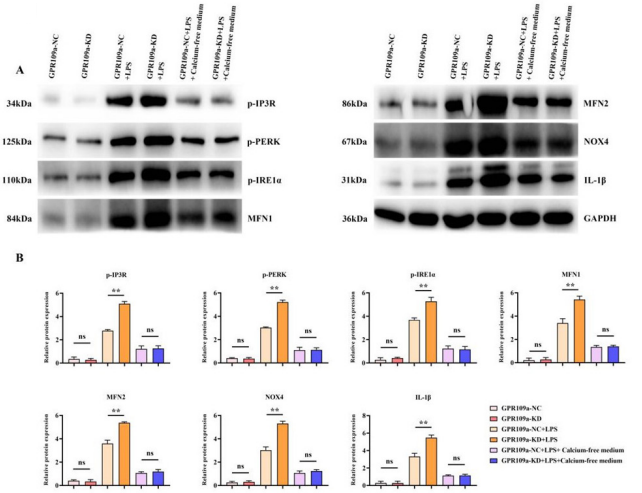


*$P$ < .01, indicating that the GPR109a-NC+LPS group's protein expression levels of p-IP3R, p-PERK, p-IRE-1α, MFN1, MFN2, NOX4, and IL-1β were significantly lower than that of GPR109a-KD+LPS group

**Abbreviations:** GPR109a, G protein-coupled receptor 109a; IL-1β, interleukin-1 beta; KD, knockdown; LPS, lipopolysaccharide; MFN1, mitofusin 1; MFN2, mitofusin 2; NC, infection control; ns, no significance; NOX4, nicotinamide adenine dinucleotide phosphate (NADPH) oxidase 4; ns, no significance; p-IP3R, phosphorylated inositol 1,4,5-triphosphate receptor; p-IRE-1α, phosphorylated inositol-requiring enzyme1/endoplasmic reticulum to nucleus1 alpha; p-PERK, phos2phorylated protein kinase RNA-like endoplasmic reticulum kinase

stress-response proteins, including phosphorylated (p-) IP3R, p-PERK, p-IRE-1α, MFN1, MFN2, NOX2, NOX4, TNF-α, and IL-1β, all significantly higher than the NC (all $P$ < .01). These findings indicate that GPR109a expression may counteract inflammatory responses, potentially through the modulation of these proteins in macrophages. (Figure 3A,B)

### Linkage Between GPR109a, Inflammation, and Ca2+ Homeostasis

Immunofluorescence studies presented that the relative fluorescence intensities indicative of inflammation-related responses were subdued in both the GPR109a-NC and KD groups, with no significant disparities ($P$ > .01). However, upon challenge with lipopolysaccharide (LPS), the NC group exhibited significantly higher fluorescence than the KD group treated with LPS ($P$ < .01), suggesting that GPR109a may play a role in enhancing the macrophage response to inflammatory stimuli through Ca2+ modulation. Interestingly, the difference was abolished when the groups were subjected to a calcium-free medium, illustrating the Ca2+ dependency of the observed effects. (Figure 4)

Additionally, Western blot indicated that the activation of inflammatory proteins was mitigated in the GPR109a-NC+LPS group as compared to the GPR109a-KD+LPS group across several markers (all $P$ < .01). This further corroborates the anti-inflammatory influence of GPR109a and suggests its regulatory role against Ca2+-induced oxidative stress pathways. (Figure 5)

### GPR109a's Role in Mitigating ER Stress and Mitochondrial Pathways

The findings detailed in Figures 5 and 6 highlight the attenuation of ER stress and modifications in mitochondrial pathways linked to inflammation in the GPR109a-NC versus the KD groups. Despite LPS stimulation, GPR109a expression appeared to protect against the over-expression of proteins associated with ER stress (p-IP3R, p-PERK, p-IRE-1α) and mitochondrial dysfunction (MFN1, MFN2, NOX4), as well the inflammatory cytokine IL-1β, suggesting a moderating effect of this receptor on such pathways. The use of 2-APB, which mitigates calcium deregulation, did not result in discernible differences between the NC and KD groups

treated with LPS, aligning with the above findings on the Ca2+ dependency of GPR109a-mediated effects. (Figure 6)

Each result collectively underscores the multifaceted role of GPR109a in diminishing inflammatory processes, improving the structural integrity of the colon, and modulating cellular responses to stress, providing valuable insights into its therapeutic potential.

## DISCUSSION

In this meticulous investigation, researchers meticulously crafted a colitis paradigm facilitated by the administration of DSS to unravel the therapeutic potential encoded within the GPR109a signal. The exploration unearthed compelling evidence that bolstered the pulsation of GPR109a, which can catalyze anti-inflammatory prowess within colonic dendritic cells and macrophages, effectively stalling the advance of colitis. These findings align harmoniously with the seminal insights contributed.[15] To deepen their understanding, the team ingeniously developed a mouse mimetic of ulcerative coloproctitis. A dual-group approach was adopted, treatment for the infection control cohort utilized a benign control virus while the knockdown faction was administered with a lentivirus encoded with a GPR109a disruption sequence.

The subsequent analysis was poignantly revealing. With the aid of Hematoxylin and Eosin (HE) staining techniques, the cellular architecture of the colonic tissues in the GPR109a-NC (negative control) group showcased a notably healthier structural integrity compared to the GPR109a-KD (knockdown) group. Delving deeper, transmission electron microscopy illuminated that cells of the GPR109a-NC group boasted robust endoplasmic reticulum (ER) and mitochondria, in distinct contrast to the deteriorated MAM structures—a soul-stirring juxtaposition to the GPR109a-KD assemblage, where proximity between the ER and mitochondria gave rise to an abundance of MAM formations.

Protein expression patterns gleaned from the GPR109a-KD cells distinctly lagged behind their GPR109a-NC counterparts, particularly after the flow cytometric isolation of CD68+ cells, which hinted at a remarkable downregulation in the GPR109a-KD faction. Protein participators such as p-IP3R, p-PERK, p-IRE-1α, MFN1, MFN2, NOX2, NOX4, TNF-α, and IL-1β, surged in the GPR109a-KD group, delivering a subtle narrative on the criticality of GPR109a in dampening the ulcerative colitis's furious march in murine models by manipulating macrophage protein expression and safeguarding ER and mitochondrial health.

The study's trailblazing pathway lays the foundation for an avant-garde analysis, leaving previously trodden paths in its academic wake. The strategic suppression of gpr109a and slc5a8 genes, responsible for encoding respective butyrate receptors and transporter, provoked a whirlwind of genetic responses tied to multifarious inflammatory cascades—including the iNOS pathway in mouse colonic epithelial cells—in a striking real-time, in vivo milieu. Parallel in vitro experiments shone a light on butyrate's remarkable prowess to impede STAT1 activation triggered by IFN-γ, which, in turn, handcuffs the upsurge of iNOS in human-derived colonic epithelial and carcinoma cells. This dual-barreled approach of butyrate, involving T cell apoptosis and the quelling of IFN-γ-driven inflammation, erects a bulwark against colonic inflammation.[16]

GPR109A, a dietary fiber-responsive beacon, ushers in gastrointestinal harmony through its deft orchestration of inflammasome activities.[17] This project's zest for precision saw the amalgamation of more evolved experimental methodologies than seen in analogous inquiries. With electron microscopy bringing ultrastructural nuances to light, and Western blot assays delineating the dynamics of pathway-specific proteins, the researchers elevating their findings to match the era's scientific fervor.

Crowning this ensemble of insights is the revelation that GPR109a engages in a complex ballet, amassing Ca2+ within macrophages whilst concurrently tempering oxidative stress, an elegant endgame in the inflammation suppression saga,

**Figure 6.** Mitigation of Inflammatory Development In Vitro via Inducement of Regulatory Protein Expression by GPR109a and the Consequent Activation of the Ca2±Stimulated Oxidative Stress Pathway. Figure 6A displays the Western blot assay results, which gauge the levels of specific proteins within the macrophages from varying murine experimental groups. Figure 6B provides a graphical representation of the quantitative expression data for these proteins among the different groups of macrophages, presented as means ± standard deviations.

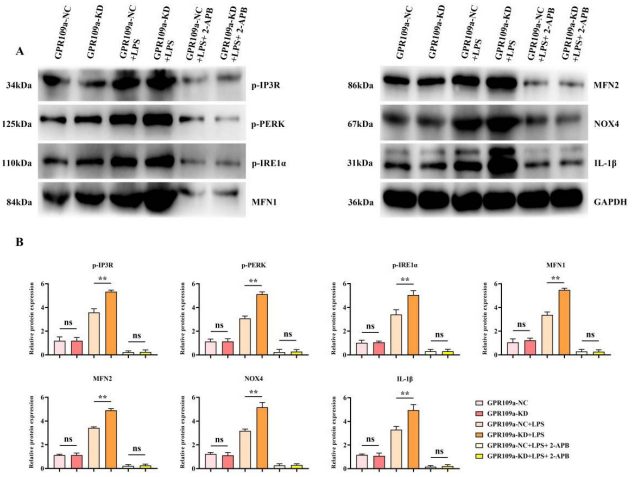


*$P < .01$, indicating that the GPR109a-NC+LPS group's protein expression levels of p-IP3R, p-PERK, p-IRE-1α, MFN1, MFN2, NOX4, and IL-1β were significantly lower than that of GPR109a-KD+LPS group

**Abbreviations:** 2-APB, 2-aminoethyl diphenyl borinate; GPR109a, G protein-coupled receptor 109a; IL-1β, interleukin-1 beta; KD, knockdown; LPS, lipopolysaccharide; MFN1, mitofusin 1; MFN2, mitofusin 2; NC, infection control; ns, no significance; NOX4, nicotinamide adenine dinucleotide phosphate (NADPH) oxidase 4; p-IP3R, phosphorylated inositol 1,4,5-triphosphate receptor; p-IRE-1α, phosphorylated inositol-requiring enzyme1/endoplasmic reticulum to nucleus1 alpha; p-PERK, phos2phorylated protein kinase RNA-like endoplasmic reticulum kinase

potentially paving the way for novel interventions in the fight against inflammatory maladies.

The orchestration of immune responses by GPR109a doesn't cease with simple anti-inflammatory action; it extends to the choreography of cellular crosstalk that is critical in re-establishing homeostasis. As the study identifies, this G-protein coupled receptor plays a pivotal role in mediating butyrate's protective effects, undeniably a sentinel in guarding the integrity of the gut barrier. The revelation that GPR109a manages to elevate intracellular Ca2+ levels in macrophages is a tour de force, shedding light on how metabolic pathways are intertwined with immune modulation. By curbing oxidative stress, GPR109a exhibits a guardian-like role, safeguarding cellular components from the collateral damage that could lead to exacerbation of the inflammatory state.

The current body of work, therefore, extends beyond a simple validation of GPR109a's role—it elucidates the multilayered mechanisms by which dietary elements and host microbiota interplay to protect and heal. Through the lens of stringent experiments, insights into organelle health and protein pathways have been crystallized, allowing us to perceive the nuanced interactions within cellular environments that could hold keys to groundbreaking therapeutic strategies.

In conclusion, this pioneering study blazes new trails in intestinal research. It meticulously underscores the potency of GPR109a modulation in mitigating ulcerative colitis, fostering an intricate balance between pro-inflammatory and antioxidative systems within the colonic microenvironment. The use of virus-mediated gene knockdown to dissect the fundamental processes relevant to colitis progression highlights the sophistication and targeted precision that underlies contemporary scientific inquiry.

By leveraging state-of-the-art technologies such as electron microscopy and Western blotting, the study does more than merely sketch a narrative of inflammation—it paints a vivid picture of cellular resilience and the capacity for recovery. It's a testament to the power of molecular science to unravel the complex tapestry of disease and to offer hope for more effective, personalized, and nuanced treatments for patients grappling with the ravages of inflammatory bowel diseases. This seminal research, promisingly, offers a beacon that shines towards a future where the management and understanding of colitis could be dramatically transformed.

## CONCLUSIONS

GPR109a can inhibit the progression of UC in mice by inducing a Ca2+-induced oxidative stress cascade in macrophages. This finding may provide some value for elucidating the mechanism of GPR109a on UC in mice and is worthy of further study.

### DECLARATION OF COMPETING INTEREST

The authors declare that they conducted the research in the absence of any competing financial interests or personal relationships that could be construed as potential conflicts of interest.

## REFERENCES


1. Asakura H. [The concept, criteria for diagnosis, and disease classification of ulcerative colitis]. *Jpn J Clin Med*. 1999;57(11):2415-2419. PMID:10572403
2. Sun Y, Zhang Z, Zheng CQ, Sang LX. Mucosal lesions of the upper gastrointestinal tract in patients with ulcerative colitis: A review. *World J Gastroenterol*. 2021;27(22):2963-2978. doi:10.3748/wjg.v27.i22.2963
3. Saito S, Mori K. Detection and Quantification of Calcium Ions in the Endoplasmic Reticulum and Cytoplasm of Cultured Cells Using Fluorescent Reporter Proteins and ImageJ Software. *Bio Protoc*. 2023;13(16):e4738. doi:10.21769/BioProtoc.4738
4. Lei Y, Chen Y, Lin Z, Tian D, Han P. Comprehensive analysis of key biomarkers, immune infiltration and potential therapeutic agents for ulcerative colitis. *Life Sci*. 2020;260:118437. doi:10.1016/j.lfs.2020.118437
5. Blas-Valdivia V, Franco-Colín M, Rojas-Franco P, Chao-Vazquez A, Cano-Europa E. Gallic Acid Prevents the Oxidative and Endoplasmic Reticulum Stresses in the Hippocampus of Adult-Onset Hypothyroid Rats. *Front Pharmacol*. 2021;12:671614. doi:10.3389/fphar.2021.671614
6. Trouvé P, Férec C, Génin E. The Interplay between the Unfolded Protein Response, Inflammation and Infection in Cystic Fibrosis. *Cells*. 2021;10(11):2980. doi:10.3390/cells10112980
7. Andruska ND, Zheng X, Yang X, et al. Estrogen receptor α inhibitor activates the unfolded protein response, blocks protein synthesis, and induces tumor regression. *Proc Natl Acad Sci USA*. 2015;112(15):4737-4742. doi:10.1073/pnas.1403685112
8. Zhao Y, Jiang Y, Chen L, et al. Inhibition of the endoplasmic reticulum (ER) stress-associated IRE-1/XBP-1 pathway alleviates acute lung injury via modulation of macrophage activation. *J Thorac Dis*. 2020;12(3):284-295. doi:10.21037/jtd.2020.01.45
9. Volkmann K, Lucas JL, Vuga D, et al. Potent and selective inhibitors of the inositol-requiring enzyme 1 endoribonuclease. *J Biol Chem*. 2011;286(14):12743-12755. doi:10.1074/jbc.M110.199737
10. Hou S, Wang L, Zhang G. Mitofusin-2 regulates inflammation-mediated mouse neuroblastoma N2a cells dysfunction and endoplasmic reticulum stress via the Yap-Hippo pathway. *J Physiol Sci*. 2019;69(5):697-709. doi:10.1007/s12576-019-00685-6
11. Zhang K, Ji X, Song Z, et al. Butyrate Inhibits Gastric Cancer Cells by Inducing Mitochondriamediated Apoptosis. *Comb Chem High Throughput Screen*. 2023;26(3):630-638. doi:10.2174/1386207325666220720114642
12. Tang H, Lu JY, Zheng X, Yang Y, Reagan JD. The psoriasis drug monomethylfumarate is a potent nicotinic acid receptor agonist. *Biochem Biophys Res Commun*. 2008;375(4):562-565. doi:10.1016/j.bbrc.2008.08.041
13. Wadie W, Mohamed SS, Abd El-Haleim EA, Khayyal MT. Niacin modulates depressive-like behavior in experimental colitis through GPR109A-dependent mechanisms. *Life Sci*. 2023;330:122004. doi:10.1016/j.lfs.2023.122004
14. Gaidarov I, Chen X, Anthony T, Maciejewski-Lenoir D, Liaw C, Unett DJ. Differential tissue and ligand-dependent signaling of GPR109A receptor: implications for anti-atherosclerotic therapeutic potential. *Cell Signal*. 2013;25(10):2003-2016. doi:10.1016/j.cellsig.2013.06.008
15. Wang F, Wang K, Xu W, et al. SIRT5 Desuccinylates and Activates Pyruvate Kinase M2 to Block Macrophage IL-1β Production and to Prevent DSS-Induced Colitis in Mice. *Cell Rep*. 2017;19(11):2331-2344. doi:10.1016/j.celrep.2017.05.065
16. Zimmerman MA, Singh N, Martin PM, et al. Butyrate suppresses colonic inflammation through HDAC1-dependent Fas upregulation and Fas-mediated apoptosis of T cells. *Am J Physiol Gastrointest Liver Physiol*. 2012;302(12):G1405-G1415. doi:10.1152/ajpgi.00543.2011
17. Macia L, Tan J, Vieira AT, et al. Metabolite-sensing receptors GPR43 and GPR109A facilitate dietary fibre-induced gut homeostasis through regulation of the inflammasome. *Nat Commun*. 2015;6(1):6734. doi:10.1038/ncomms7734